Journal of Physics: Conference Series

Numerical Simulations of the flow field within a 1:10 Aspect Ratio duct at intermediate Re

Numerical Simulations of the flow field within a 1:10 Aspect Ratio duct at intermediate Re

Federica VIGNATI, Damiano FUSTINONI, Pasqualino GRAMAZIO, Luigi VITALI and Alfonso NIRO

Dipartimento di Energia, Politecnico di Milano, Milan, Italy

E-mail: alfonso.niro@polimi.it

Abstract. Numerical simulations are carried on to study the fluid-dynamical features of a smooth duct with aspect ratio of 10. The duct is operated with an incompressible, newtonian fluid, whose Reynolds number, computed over the hydraulic diameter and bulk velocity, ranges from 470 to 14500, encompassing laminar and turbulent flow. To capture the details of all the flow scales, Direct Numerical Simulations are performed, by means of a code developed at Politecnico di Milano. The adopted code is a finite-difference, structured grid solver, that includes a mass flow rate correction. The latter guarantees high accuracy in the calculation of unsteady flows, or during the transition to turbulent regime, and it allows to check the consistency of numerical results.

Both global parameters –including the friction factor and the identification of the laminar-to-turbulent transition and local flow features, e.g., corner vortexes, are investigated and presented in this work. Preliminary analyses agree fairly well with literature data and with experimental results obtained at ThermALab of Politecnico di Milano.

The final goal of this work, including a deep integration between the numerical and the experimental setup, is to carry on detailed investigations of the fluid-dynamical and thermal characteristics of ribbed ducts, in the perspective of heat transfer enhancement and pressure drop reduction.

1. Introduction

As it is well known, the main factor for the enhancement of convective heat transfer is the flow Reynolds number, which represents the influence of turbulence [1]. Unfortunately, a study of the latter still represents a difficult task, due to the phenomena complexity. For this reason, numerical studies represent an interesting tool for the investigation of fluid-dynamical details [2–6]. The flow in a rectangular duct with smooth walls and an Aspect Ratio (AR) of $1:10$ is investigated by means of Direct Numerical Simulations (DNS). To limit the computational cost of the simulations, the Reynolds number is limited to 14500, which has not been deeply investigated yet, aiming at providing a first assessment on the flow details.

In most scientific studies, some assumptions are adopted, to reduce the computational burden in case of numerical studies, the complexity of the equations for theoretical approaches, or the facility size for experimental works. In particular, in the first two approaches the flow is often assumed to be fully-developed, to neglect the modeling of the laminar-turbulent transition, if any, and to reduce the computational domain size. This hypothesis is often reasonable, as the length of several experimental facilities or industrial components allows to neglect inlet

effects [6, 7]. Moreover, in several works, the flow is also assumed to be homogeneous in the spanwise direction, i.e. statistically two-dimensional. This feature is very useful especially when numerical investigations are carried out, as it allows to overcome the difficulties of imposing exact boundary conditions on lateral walls [8] and to adopt more efficient and accurate computational techniques, e.g. spectral methods [3,6]. For a long time, it has been considered possible to apply the two-dimensional hypothesis also to duct flows with a moderate aspect ratio [9–11], but more recent studies have demonstrated that non-negligible three-dimensional effects arise for aspect ratios up to 24, at least [12–15]. For this reason, special care must be adopted when comparing numerical, experimental and theoretical results, to make sure to be comparing data obtained in similar operating conditions.

This work stems from the need to support experimental results obtained during a long-term campaign carried out at the ThermALab of Energy Department of Politecnico di Milano, on the enhancement of heat transfer in forced convection of air flows through rectangular channels by means of square ribs in a large variety of geometrical configurations. The ribs are adopted to promote turbulence, by inducing secondary flows of the second type [16, 17] as well as by destabilizing the boundary layer growth. The program goal is to find optimal rib configurations, associated to the best compromise between heat transfer enhancement and pressure drop penalty.

2. Numerical simulations setup

2.1. Numerical model

The investigated duct features are summarized in table 1. All data refer to the experimental apparatus of ThermALab, that was investigated in previous works and that is used as benchmark for the presented numerical results. The experimental facility necessarily includes an inlet part, where the flow is not developed. For this reason the length of the fully-developed flow region (1000 mm) is lower than the overall duct length (2400 mm). In numerical simulations, only the fully-developed flow region is considered, defined L_x.

Table 1. Main duct geometric parameters and operational conditions.

Channel half-height	δ	6.0 mm
Channel length (streamwise)		2400.0 mm
Channel length (developed flow)	L_x	1000.0 mm
Channel width (spanwise)	L_y	120.0 mm
Hydraulic diameter, D_h	$4 \cdot (\delta L_y / 2\delta + L_y)$	21.82 mm
Aspect ratio	$AR = L_y / 2\delta$	10

The Reynolds number Re_D, defined over the hydraulic diameter D_h, the bulk velocity U_b and the kinematic viscosity ν, ranges from 470 to 14500. The interest in the combination between the selected combination of Re_D and AR is twofold: on the first hand, it represents a little-investigated configuration, whereas a number of industrial applications, e.g., air solar heaters [18, 19], work in these operational conditions. On the second hand, it encompasses laminar, transitional and turbulent flow regimes in presence of Prandtl's secondary flows [16,17], whereas, for a long time, three-dimensional effects have often been neglected in ducts characterized by $AR = 10$.

2.2. Features of the simulations

The numerical simulations are performed by solving three-dimensional, unsteady, incompressible [20] Navier-Stokes equations, by means of a Compact Finite Difference scheme. The adopted

software uses a DNS (Direct Numerical Simulations) approach, and therefore there is no need to implement, tune and set a numerical model for turbulence. The numerical equations are made dimensionless with the duct half-height δ and the bulk velocity, and therefore, in the following, all quantities will be expressed in terms of dimensionless values. The laboratory duct is operated with air, but compressibility is neglected due to the very low flow velocities. Therefore, a velocity-pressure coupling is needed, which is provided by means of the Laplace equation solution [21]. The code was developed at Politecnico di Milano for the simulation of channel flows, and later adapted by the authors to simulate duct flows, as well [22, 23].

Boundary conditions are of no-slip and non-penetration types on the non-homogeneous directions, i.e., duct height y and spanwise z, resulting in zero-velocity and zero-derivative of the pressure in the wall-normal direction [8]. To refer to fully developed flows, periodic boundary conditions are applied to both the velocity and the pressure field in the streamwise direction x [6, 7, 24, 25].

The simulation, regardless of the flow Reynolds number, are initialized with the solution for the laminar flow, $\mathbf{u} = (u, 0, 0)$, where the streamwise velocity u is known [26] and results from the analytic solution of Navier-Stokes equations under the assumptions of uniform pressure and zero-velocity components v and w in non-streamwise directions y and z. A random perturbation, depending only on the time-step value, is then added during the first time steps to the laminar solution: if the Reynolds number is sufficient, the transitions to turbulence occurs, whereas, for low Reynolds numbers, the viscosity damps the perturbations, recasting the flow to laminar conditions [7, 27–30]. Both the node spacing and the time step are chosen in accordance to [25], to resolve all the flow scales. The fixed grid is refined near the walls and the corners to increase the accuracy. To assure the conservation of the mass flow rate during the initial transient, a technique formulated for channel flow simulations [31] is adapted to compute duct flows and implemented: this allows to both prevent non-physical oscillations and to compute the friction factor, as duly described in [23].

Space and time discretization is performed in accordance to most literature works, e.g., [6, 7, 25], and it depends on the considered Reynolds number. In the most critical case, the simulations are designed to make sure that the distance from the wall and the first node remains below 0.1 (in viscous units), and gradually increased while moving towards the duct core. A uniform and coarser space discretization is applied in the streamwise (homogeneous) direction. The time step is computed to keep the CFL number below 0.5 [32]. For additional details on the space discretization, time step setting and numerical scheme, the reader is addressed to [6, 7, 22, 23, 25].

The adopted code derives from the well validated one [22, 33] dedicated to the simulation of channel flow. To verify the capability of the code to tackle three dimensional effects, numerical results have been compared with experimental data [23] and literature results [12–15].

3. Results

Figure 1 shows two profiles of the velocity field u component along the duct height, computed for 1(a) $Re = 2036$ and 1(b) $Re = 10180$, depicting the typical mean laminar and turbulent behaviours. The profiles have been obtained after a time averaging (over 60 and 1000 time units, respectively) of instantaneous flow fields, and two space averagings, over the homogeneous direction x and the spanwise direction z. The regularity of the profiles is an indicator of a good choice of the total length of the simulations, in accordance also with [12]. Of course, since laminar flows are also stationary, a shorter time is sufficient.

3.1. Instantaneous flow fields

Instantaneous velocity intensity fields $\sqrt{u^2 + v^2 + w^2}$, computed at the last simulated time and at the inlet section, are shown in figure 2, for Reynolds numbers of 2(a) 470, 2(b) 3636, 2(c)

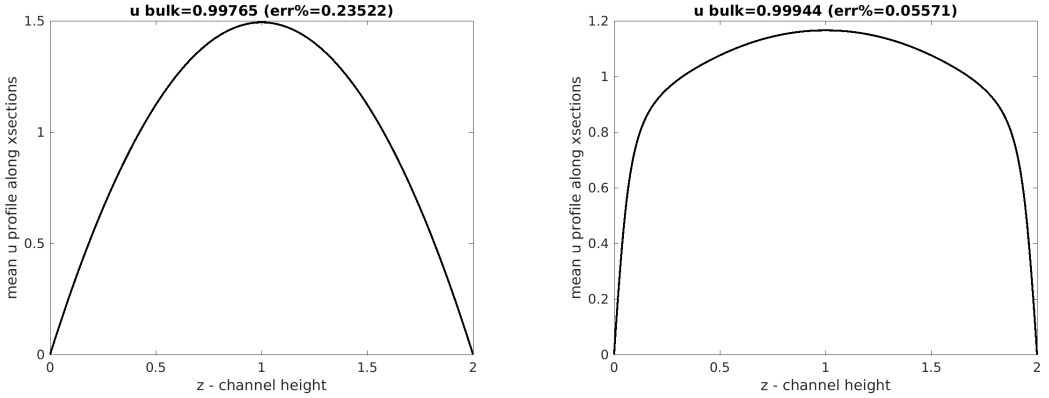

(a) (b)

Figure 1. Distribution along the channel height of the u velocity component, averaged along time, x and y directions, showing high similarity with the well known profiles in channel flows in (a) laminar ($\mathrm{Re_D} = 2036$) and (b) turbulent flows ($\mathrm{Re_D} = 10180$).

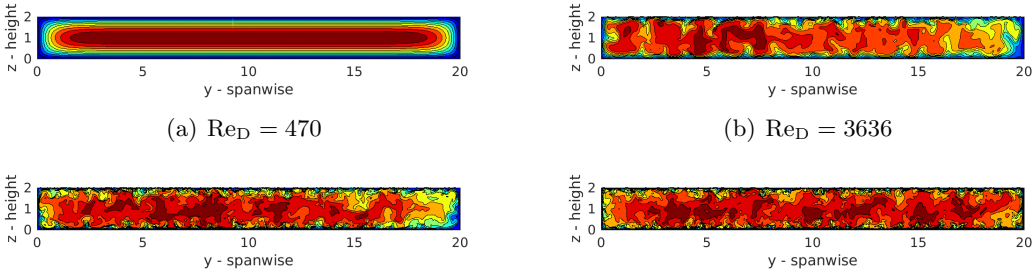

(a) $\mathrm{Re_D} = 470$ (b) $\mathrm{Re_D} = 3636$

(c) $\mathrm{Re_D} = 7272$ (d) $\mathrm{Re_D} = 10180$

Figure 2. Instantaneous velocity magnitude in a cross-stream section, at the last simulated time for 2(a) $\mathrm{Re_D} = 470$, 2(b) $\mathrm{Re_D} = 3636$, 2(c) $\mathrm{Re_D} = 7272$ and 2(d) $\mathrm{Re_D} = 10180$. Blue and ruby represent respectively the minimum and the maximum values (as in the following figures), ranging from zero to approximately twice U_b, depending on the considered $\mathrm{Re_D}$.

7272, and 2(d) 10180. An increasing complexity of the flow field is observed, associated with larger Reynolds numbers and, therefore, smaller scales. For the $\mathrm{Re_D} = 10180$ case, in particular, according to [15], the average size of near-wall streaks is of approximately 100 wall units, on both pairs of walls.

3.2. Detection of the transition

Figure 3, extracted from [23], depicts Fanning friction f_F factors (which corresponds to one-fourth of the well known Darcy friction factor) computed by means of DNS calculations, and compared to experimental data. The laminar-to-turbulent regime transition is well detected, and agrees fairly well with literature data. The discrepancies between numerical and experimental results, in terms of both transitional Reynolds numbers and of f_F value, are attributed to two reason. On the first hand, the features of the test apparatus (described in [23]), which is equipped with a smooth inlet diffuser, which is known to possibly trigger a late transition to turbulence [34]. On the other hand, the location of the probes (at the centerline) which is less sensitive than numerical techniques to three-dimensional effects on f_F.

The comparison between the Fanning friction factor f_F-detected transitional $\mathrm{Re_D}$ and the

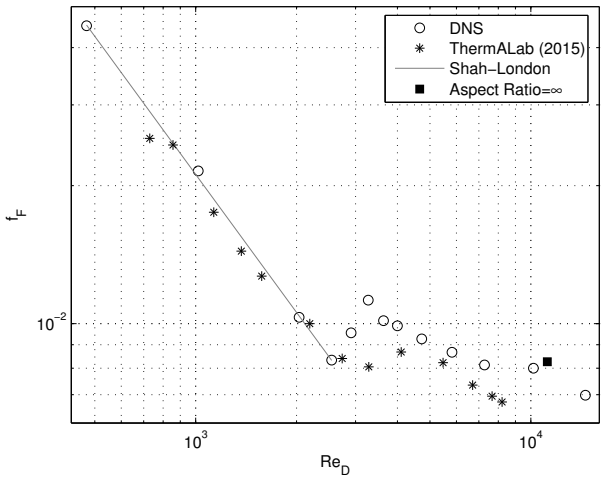

Figure 3. DNS and experimental results obtained at ThermALab of PoliMi for the Fanning friction factor of a duct flow with $AR = 10$ at $\mathrm{Re_D}$ between 470 and 14500 [23].

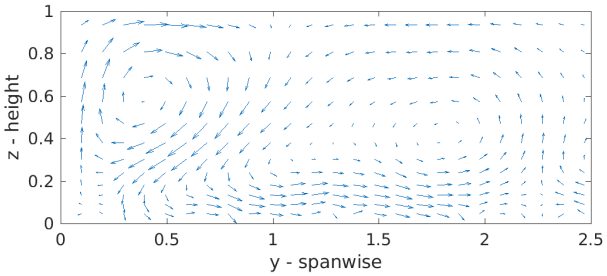

Figure 4. Secondary-flows-induced corner vortexes represented as vectors of time- and streamwise-averaged velocity components $\overline{v}$ and $\overline{w}$.

computed flow fields (see, e.g., figure 2) shows good accordance.

3.3. Corner vortexes

Figure 4 highlights corner vortexes as vectors of components $\overline{v}$ and $\overline{w}$ in the streamline-normal cross-section. These two velocity components represent v and w averaged with respect to x and time, since corner vortexes cannot be observed on instantaneous flow fields, but are statistical features only [15]. The rightmost vortex is stretched in the spanwise direction, as predicted by [15], due to the large duct aspect ratio.

The effect of these vortexes is to convect momentum from the core to the edges of the duct (along the corner bisectors) or, conversely, in the opposite direction (along the walls, relatively far from the corners), as confirmed also by [35] and [36]. The contribution of corner secondary flows to the overall momentum is not very significant in terms of numerical values, if compared to, e.g., the streamwise component, but it strongly affects $\overline{u}$, that is the time- and streamwise-averaged distribution of u, locally reversing the isotech-line ($\overline{u}$-contour) concavity with respect to the laminar case. This effect is well visible by comparing figures 5(a) and 5(b), which represent $\overline{u}$ for $\mathrm{Re_D} = 1018$ (laminar) and $\mathrm{Re_D} = 7272$ (turbulent), respectively, and therefore influences the Fanning friction factor, which depends on the mean wall-normal derivatives of $\overline{u}$ [23].

3.4. Kinetic energy

The corner vortexes can be identified also by observing the kinetic energy of the mean secondary flows, $K = (\overline{v}^2 + \overline{w}^2)/2$, which is depicted in figure 6 for the two turbulent flows at $\mathrm{Re_D} = 3636$ and $\mathrm{Re_D} = 5818$, respectively. Albeit the map for $\mathrm{Re_D} = 5818$ agrees fairly well with literature ones (at least qualitatively, as $\mathrm{Re_D}$ is different), an unexpected peak is observed at the duct half-height, near the side wall, for the $\mathrm{Re_D} = 3636$-case. This is probably due to the low value of $\mathrm{Re_D}$, which does not identify fully-developed turbulent conditions, and therefore may possibly show different flow features.

Eventually, in accordance to the procedure developed in [15], the duct is subdivided into 20

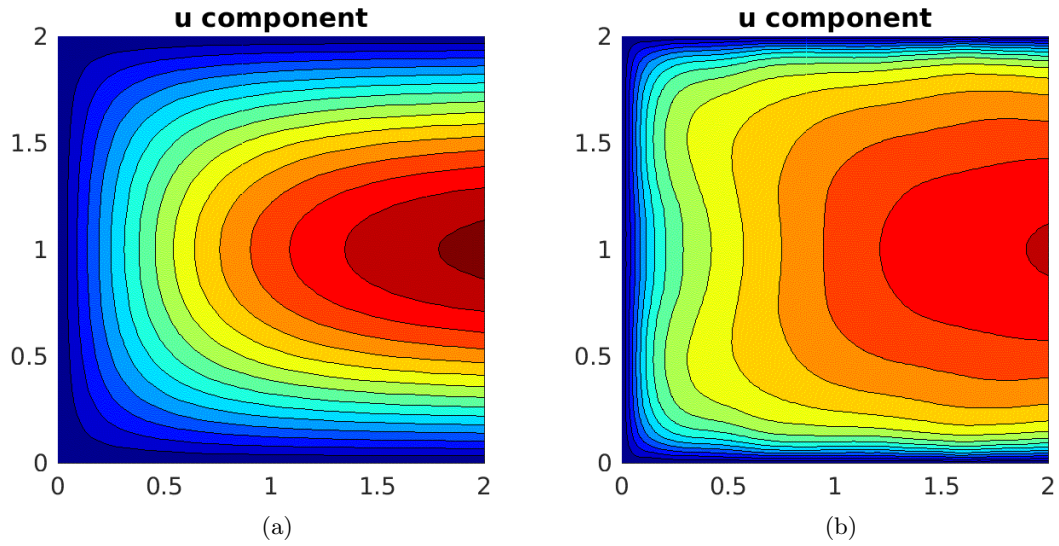

Figure 5. Map of the time- and streamwise-averaged u component, magnified in correspondence of the corner, for (a) $\mathrm{Re_D} = 1018$ (laminar) and (b) $\mathrm{Re_D} = 7272$ (turbulent). $\overline{u}$ ranges from zero (blue areas) to approximately 1.6 (ruby areas), depending on the considered $\mathrm{Re_D}$. The difference between the regular profiles of the laminar case and the locally-reversed concavity of the isotech lines ($\overline{u}$ contours) is evident.

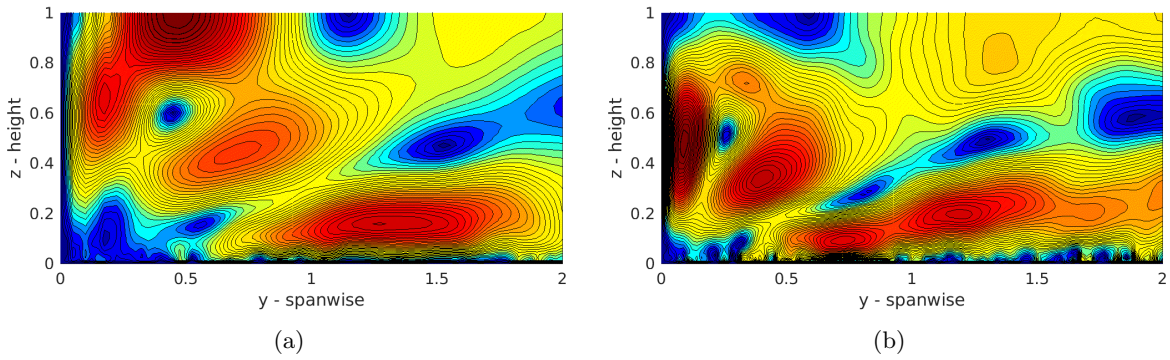

Figure 6. Kinetic energy of the secondary flows in the cross-stream plane, in correspondence of the corner. Due to the symmetry (neglecting tiny fluctuations) of the mean flow, only one corner is depicted. The Reynolds numbers are (a) 3636 and (b) 5818. K ranges from zero (blue areas) to approximately $U_b \cdot 10^{-4}$ (ruby areas), depending on the considered $\mathrm{Re_D}$.

equal regions (the so-called "windows", in [15]) in the spanwise direction, and K is evaluated on each window separately, and averaged along z. This allows to determine to what extent the lateral walls induce significant secondary flows, which are known to decrease in intensity while approaching the duct centerline. For the considered AR = 10, it is known that K is different from zero even after the flow convergence if computed within the 5δ from the lateral walls (which is commonly assumed as the maximum extent within which side walls affect the flow), whereas it presents a linear decay in time along the centerline, in accordance to channel flow behavior. For this reason, the values of K on each window are shown in figure 7, concerning the case of $\mathrm{Re_D} = 4000$, after an averaging over 1000 time units. The picture on the left refers to the

window near the duct lateral wall, and the distance from the latter increases from left to right, so that the rightmost picture concerns the duct core. According to literature [15], the mean value over the window (red line) is between 10^{-6} and 10^{-5} in the flow core, and it increases while approaching the walls (with a slight increase in the sixth window). Conversely, K in the first window is larger than the one predicted by [15], even after convergence. Both discrepancies (in the first and sixth windows) are possibly due to the low $\mathrm{Re_D}$, which corresponds to transitional regime, as for figure 6(a).

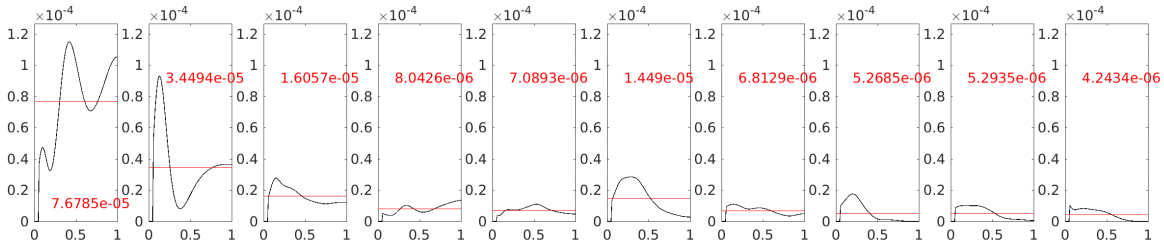

Figure 7. Kinetic energy of the secondary flows in the cross-stream plane, averaged over mobile windows, for $\mathrm{Re_D} = 4000$. The picture on the left refers to the window near the duct lateral wall, and the distance from the latter increases from left to right, so that the rightmost picture concerns the duct core.

4. Conclusions

Direct Numerical Simulations are performed to investigate the flow features in a rectangular duct with Aspect Ratio of 10. Laminar, transitional and turbulent flow are encompassed, with Reynolds numbers ranging from 470 to 14500.

This configuration is interesting, since duct flows in correspondence of the laminar-turbulent transition in ducts with AR = 10 have not been widely studied yet, but represent several industrial applications. In particular, for the considered Aspect Ratio, data agree with channel flow results when integral parameters are considered (friction factor, transitional $\mathrm{Re_D}$), but relevant differences are highlighted when the flow field is investigated, due to the presence of Prandtl's secondary flows of the second type.

DNS are carried out by means of a Finite-Difference solver for unsteay, incompressible, Navier-Stokes equations on structured grids developed at Politecnico di Milano.

The preliminary results obtained during the solver validation shows good accordance with literature data (theoretical, numerical and experimental), proving the code to be able to resolve accurately the complex flow field. The transition is correctly identified, and the two adopted criteria agree fairly well. Instantaneous and mean velocity fields are provided and analyzed, highlighting the presence, the shape and the extent of corner vortexes. An interesting behaviour is observed for Reynolds number near the transition, which should be further investigated.

Results can be extended, to provide a unique database between numerical and experimental data. It should be indeed indicated to derive a unique procedure for the evaluation of the Fanning friction factor. Moreover, the flow field in presence of ribs, as well as the temperature field in correspondence of heated walls will be investigated in the future.

References

[1] Webb R L 1994 *Principles of enhanced heat transfer* (New York: Winley-Interscience)
[2] Rodi W, Mansour N N 1993 Low Reynolds number $k-\varepsilon$ modelling with the aid of direct simulation data *J. Fluid Mech.* **250** 509
[3] Mansour N N, Kim J, and Moin P 1988 Reynolds-stress and dissipation rate budgets in a turbulent channel flow *J. Fluid Mech.* **194.15**

[4] Blackburn H M, Mansour N N and Cantwell B J 1996 Topology of fine scale motions in turbulent channel flow *J. Fluid Mech.* **310** 269
[5] Kim J and Antonia R A 1993 Isotropy of the small scales of turbulence at low Reynolds number *J. Fluid Mech.* **251** 219
[6] Kim J, Moin P and Moser R D 1987 Turbulence statistics in fully developed channel flow at low Reynolds number *J. Fluid Mech.* **177** 133
[7] Luchini P and Quadrio M 2006 A low-cost parallel implementation of direct numerical simulation of wall turbulence *J. Comput. Phys.* **211.2** 551-71
[8] Anders Petersson N 2001 Stability of Pressure boundary Conditions for Stokes and Navier–Stokes Equations *J. Comput. Phys.* **172** 40-70
[9] Dean R B 1978 Reynolds number dependence of skin frictin and other bulk flow variables in two-dimensional rectangular duct flow *J. Fluid Eng.* **100** 215
[10] Bradshaw P and Hellens G E 1964 The N.P.L. 59 in x 9 in boundary layer tunnel *N.P.L. Aero Report* **1119**
[11] Monty J P 2005 Developments In Smooth Wall Turbulent Duct Flows *PhD thesis, University of Melbourne*
[12] Vinuesa R, Noorani A, Lozano-Durán A, El Khoury G K, Schlatter P, Fischer P F and Nagib H M 2014 Aspect ratio effects in turbulent duct flows studied through direct numerical simulation *J. of Turbulence* **15.10** 677-706, doi:10.1080/14685248.2014.925623
[13] Vinuesa R 2013 Synergetic computational and experimental studies of wall-bounded turbulent flows and their two-dimensionality *PhD thesis, Illinois Institute of Technology*
[14] Vinuesa R, Bartrons E, Chiu D, Dressler K M, Rüedi J D, Suzuki Y, Nagib H M 2014 New insight into flow development and two dimensionality of turbulent channel flows *Exp. Fluids* **55** 1759 https://doi.org/10.1007/s00348-014-1759-8
[15] Vinuesa R, Schlatter P and Nagib H M 2015 Characterization of the secondary flow in turbulent rectangular ducts with varying aspect ratio *Int. Symposium on Turbulence and Shear Flow Phenomena (TSFP-9), June 30-July 3 2015, Melbourne, Australia*
[16] Prandtl L 1926 Über Die Ausgebildete Turbulenz *Proceedings 2nd International Congress Applied Mechanics, 12-17 September 1926, Zurich, CH*
[17] Prandtl L 1927 Turbulent Flow *NACA TM - 435*
[18] Deo NS, Chander S, Saini S 2016 Performance analysis of solar air heater duct roughened with multigap V-down ribs combined with staggered ribs *Renewable Energy* **91** 484-500
[19] Kumar A, Kim MH 2015 Convective heat transfer enhancement in solar air channels *Applied Thermal Engineering* **89**
[20] Shirokoff D and Rosales R R 230 An efficient method for the incompressible Navier-Stokes equations on irregular domains with no-slip boundary conditions, high order up to the boundary *J. Comput. Phys.* **230** 8619-46
[21] Gavrilakis S 1992 Numerical simulation of low-Reynolds-number turbulent flow through a straight square duct *Journal of Fluid Mechanics* **244** 101-129 doi:10.1017/S0022112092002982
[22] Monti C M 2017 Metodo dei contorni immersi per la simulazione numerica diretta di correnti turbolente su pareti non piane *MSc thesis, Politecnico di Milano*
[23] Vignati F, Gramazio P, Vitali L, Fustinoni D, Niro A 2019 Preliminary DNS results of friction factor at low Re inside a rectangular channel with 1:10 Aspect Ratio *Journal of Physics: Conference Series* **1224(1)** 012047 doi:10.1088/1742-6596/1224/1/012047
[24] Quadrio M and Luchini P 2001 A $4-th$ order accurate, parallel numerical method for the direct simulation of turbulence in cartesian and cylindrical geometries *Proc. of the XV AIMETA Conf. on Theor. Appl. Mech*
[25] Comini G, Croce G and Nobile E 2008 *Fondamenti di termofluidodinamica computazionale* (S.G.E)
[26] Shah R K and London A L 1978 *Laminar Flow Forced Convection in Ducts - A Source Book for Compact Heat Exchanger Analytical Data* (New York: Academic Press, Inc)
[27] Orszag S A 1971 Accurate solution of the Orr–Sommerfeld stability equation *J. Fluid Mech.* **50.04** 689-703
[28] Uhlmann M and Nagata M 2006 Linear stability of flow in an internally heated rectangular duct *J. Fluid Mech.* **551** 387-404 doi:10.1017/S0022112005008487
[29] Theofilis V, Duck P W and Owen J 2004 Viscous linear stability analysis of rectangular duct and cavity flows *J. Fluid Mech.* **505** 249-286 doi:10.1017/S002211200400850X
[30] Tatsumi T and Yoshimura T 1990 Stability of the laminar flow in a rectangular duct Journal of Fluid Mechanics *J. Fluid Mech.* **212** 437-449 doi:10.1017/S002211209000204X
[31] Quadrio M, Frohnapfel B, Hasegawa Y 2016 Does the choice of the forcing term affect flow statistics in DNS of turbulent channel flow? *European J. of Mech. B/Fluids* **55** 286-293
[32] Courant R, Friedrichs K, Lewy H 1967 On the partial difference equations of mathematical physics *IBM Journal of Research and Development* **11(2)** 215-234 doi:10.1147/rd.112.0215

[33] Luchini P 2016 Immersed-boundary simulations of turbulent flow past a sinusoidally undulated river bottom *European Journal of Mechanics - B/Fluids* **55.2** 340-347
[34] Hartnett JP, Koh JY, McComas ST 1962 A Comparison of Predicted and Measured Friction Factors for Turbulent Flow Through Rectangular Ducts *ASME. J. Heat Transfer* **84.1** 82-88 doi:10.1115/1.3684299
[35] Uhlmann M, Pinelli A, Kawahara G, Sekimoto A 2007 Marginally turbulent flow in a square duct *J. Fluid Mech* **588** 153-162
[36] Gessner FB 1973 The origin of secondary flow in turbulent flow along a corner *J. Fluid Mech* **58** 1-25